The use of a star-shaped trifunctional acyl chloride for the preparation of polyamide thin film composite membranes

Maaskant, Evelien; Vogel, Wouter; Dingemans, Theo J.; Benes, Nieck E.

DOI
10.1016/j.memsci.2018.09.032

Publication date
2018

Document Version
Accepted author manuscript

Published in
Journal of Membrane Science

The use of a star-shaped trifunctional acyl chloride for the preparation of polyamide thin film composite membranes

Evelien Maaskant[a], Wouter Vogel[b,c], Theo J. Dingemans[d], Nieck E. Benes[a,*]

[a] *Films in Fluids Group - Membrane Science and Technology cluster, Faculty of Science and Technology, MESA+ Institute for Nanotechnology, University of Twente, P.O. Box 217, 7500 AE Enschede, The Netherlands*
[b] *Faculty of Aerospace Engineering, Delft University of Technology, Kluyverweg 1, Delft, Netherlands*
[c] *DPI, P.O. Box 902, 5600 AX Eindhoven, The Netherlands*
[d] *Applied Physical Sciences, University of North Carolina at Chapel Hill, 121 South Rd, NC, United States*

Supporting information

Contents

*Corresponding author. n.e.benes@utwente.nl

1. NMR spectra

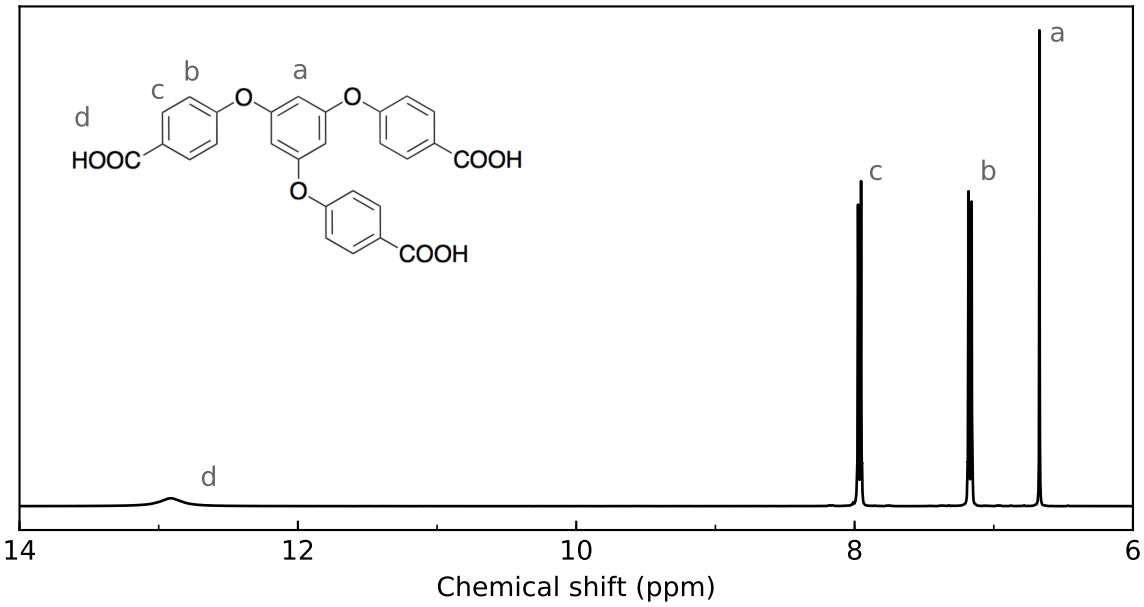

Figure 1: ^{1}H-NMR spectrum of **2** recorded in DMSO-d6.

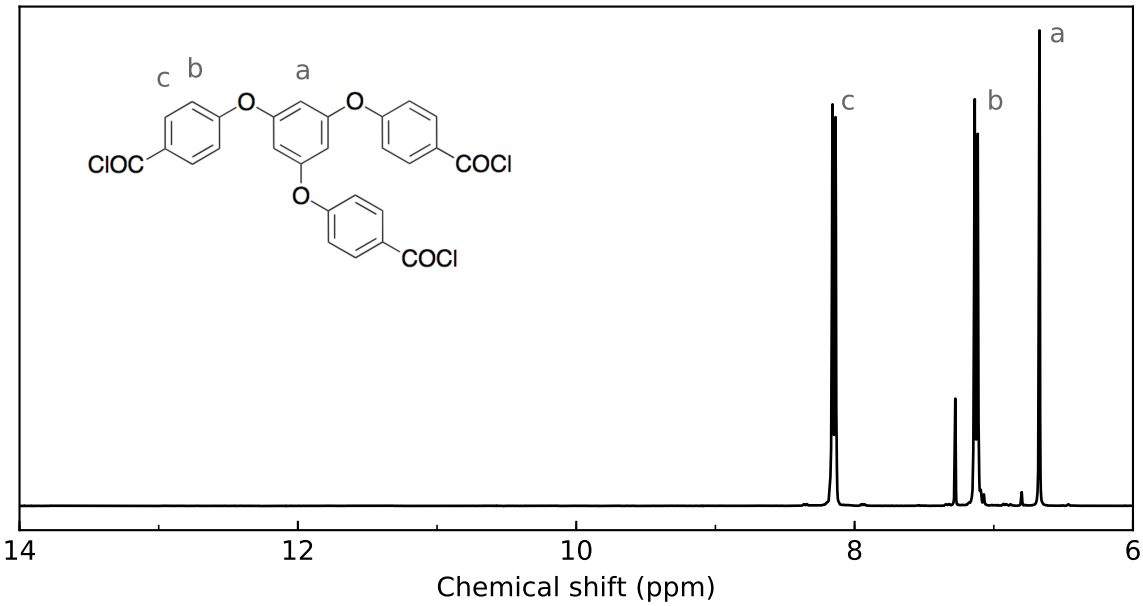

Figure 2: ^{1}H-NMR spectrum of **3** recorded in $CDCl_3$.

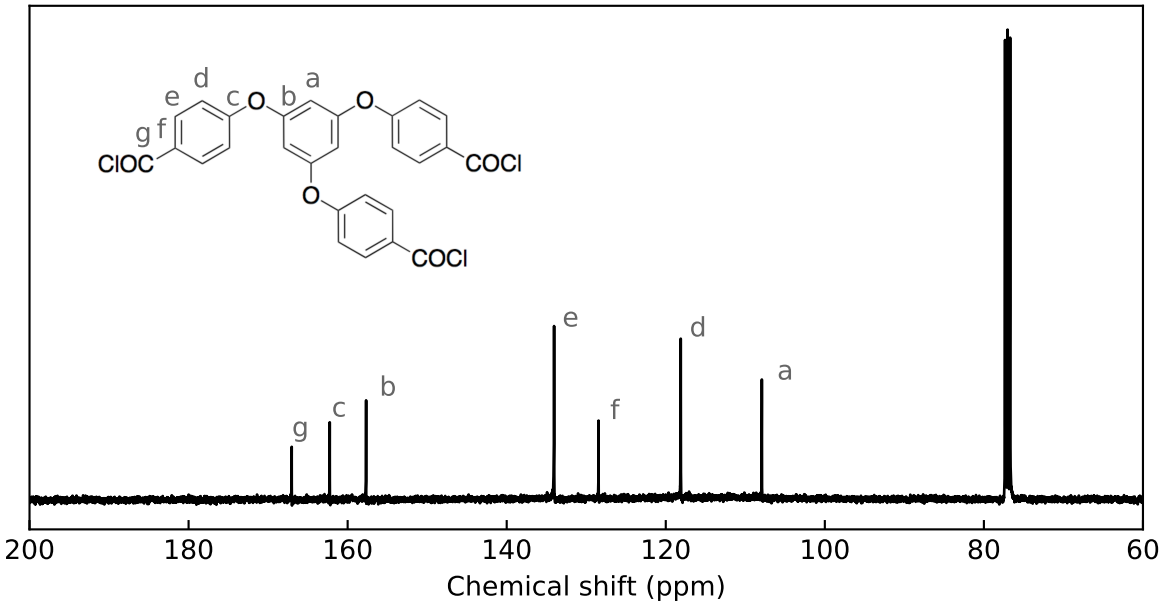

Figure 3: ^{13}C-NMR spectrum of **3** recorded in $CDCl_3$.

2. FTIR spectra

The ATR-FTIR spectra of the monomers **2** and **3** are given in Figure 4. The spectrum of **2** shows a sharp absorbance peak originating from the C=O stretching of the carboxylic acid at 1675 cm^{-1}. In addition, a broad absorbance peak is observed around 2800 cm^{-1}, which originates from the OH stretching of the carboxylic acid.

The carboxylic acid groups of **2** are converted into acyl chloride groups upon treatment with thionyl chloride ($SOCl_2$) revealing monomer **3**. The C=O stretching of the acyl chloride shifts to 1740 cm^{-1} in the spectrum of **3**.

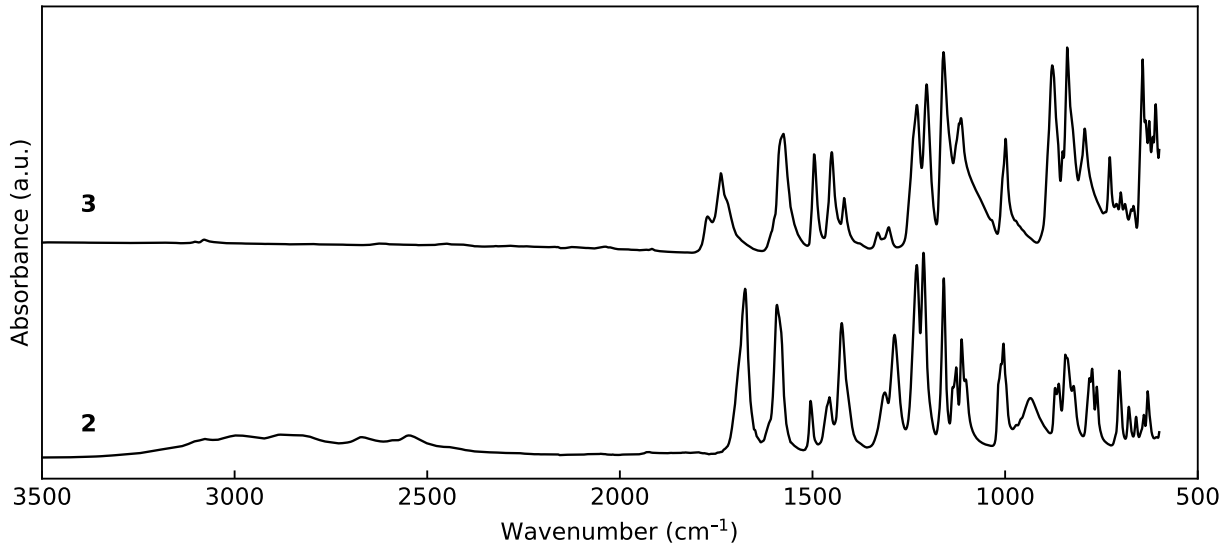

Figure 4: ATR-FTIR spectra of **2** and **3**.

3. Film thickness

The film thickness of the polyamide films prepared on silicon wafers is shown in Figure 5. All films showed to have a low light reflectivity, and therefore an extremely low intensity. In combination with a high surface roughness, the fitting of the ellipsometric spectra gives raise to a high error in these measurements.

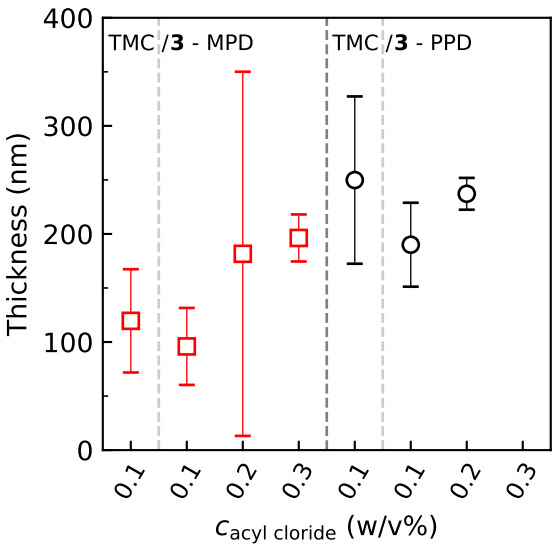

Figure 5: The film thickness of polyamide films on silicon wafers. MPD-based polyamides are represented by red squares (□), and PPD-based polyamides by black circles (○). The error bars represent the 95% confidence interval calculated from 3–5 measurements.

4. Contact angle

The contact angles of the prepared polyamide films are shown in Figure 6. Interestingly, the measured contact angle for our TMC-MPD film is much lower as compared to values reported in literature, that vary between 60–80°[1–3]. These literature values are measured on TMC-MPD films deposited on a porous polymeric support, whereas here the films are supported by a silicon wafer.

The **3**-MPD films prepared with 0.1 w/v% acyl chloride seem to have a relatively high contact angle as compared to all other polyamide films. However, all films were washed with excess water after synthesis, except for these films. Due to their fragility these films could not be washed with water, and therefore their contact angle could be overestimated.

In general, the films prepared from both **3**-MPD and **3**-PPD show to have a lower contact angle as compared to their TMC-based analogues. This is surprising, considering the increased monomer size, and thus reduced amount of amide groups per unit volume for **3**-based polyamides. The lower contact angle can be explained by a higher amount of unreacted end-groups, and thus a lower cross-linking density.

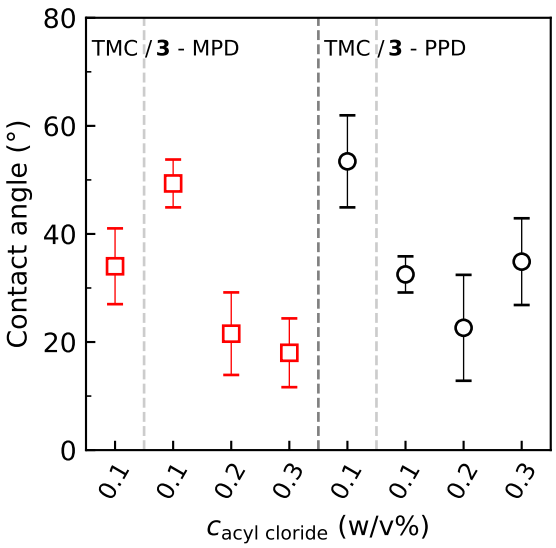

Figure 6: Contact angle of polyamide films on silicon wafers. MPD-based polyamides are represented by red squares (□), and PPD-based polyamides by black circles (○). The error bars represent the 95% confidence interval calculated from 5 measurements.

5. Thermogravimetric analysis

Figure 7 shows the mass loss as function of temperature for the monomers **2** and **3**.

The mass loss as a function of temperature and the corresponding gases evolved for polyamide powders is given in Figure 8 for MPD-based polyamides, and in Figure 9 for PPD-based polyamides.

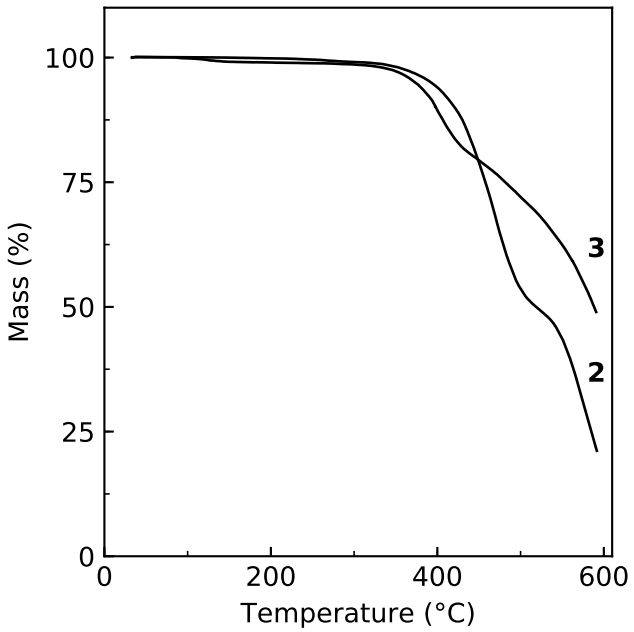

Figure 7: Mass loss as function of temperature for **2** and **3**. All traces were obtained under a nitrogen atmosphere, with a heating rate of 10 °C min^{-1}.

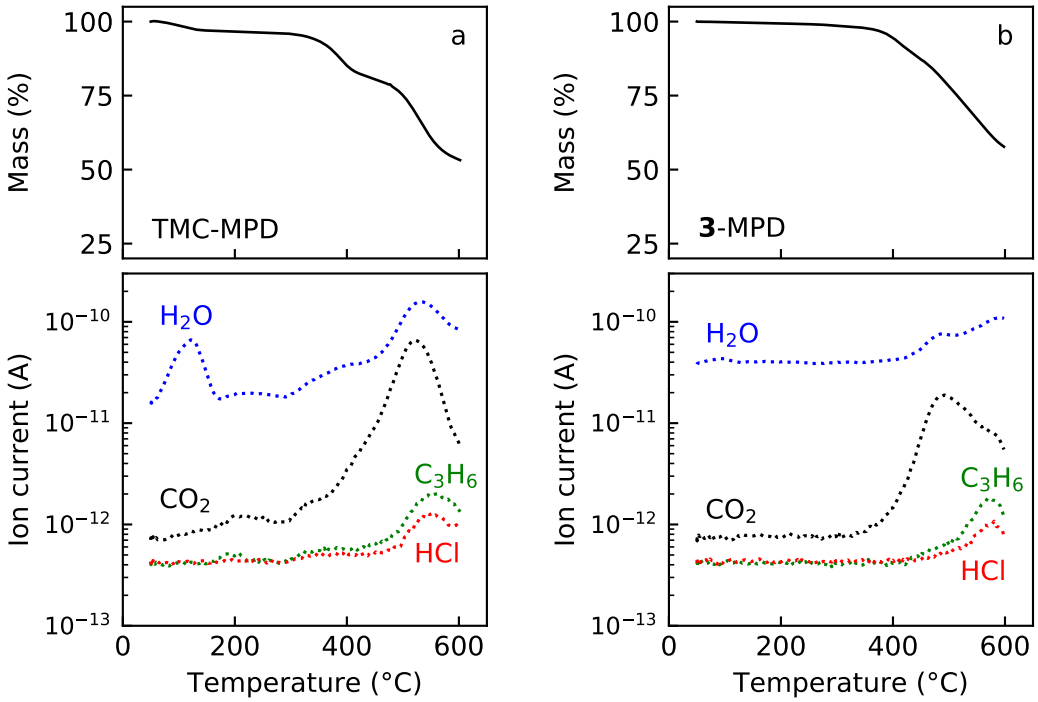

Figure 8: TGA-MS spectra of (a) TMC-MPD and (b) **2**-MPD obtained under a nitrogen atmosphere with a heating rate of 10 °C min^{-1}. The top graphs show the mass loss as function of temperature. The bottom graphs show the evolved gases. The tracked *m/z* values are H_2O (*m/z*=18, blue, —), HCl (*m/z*=38, red, —), C_3H_3 (*m/z*=39, fragment originating from aromatic ring, green, —), and CO_2 (*m/z*=44, black, —).

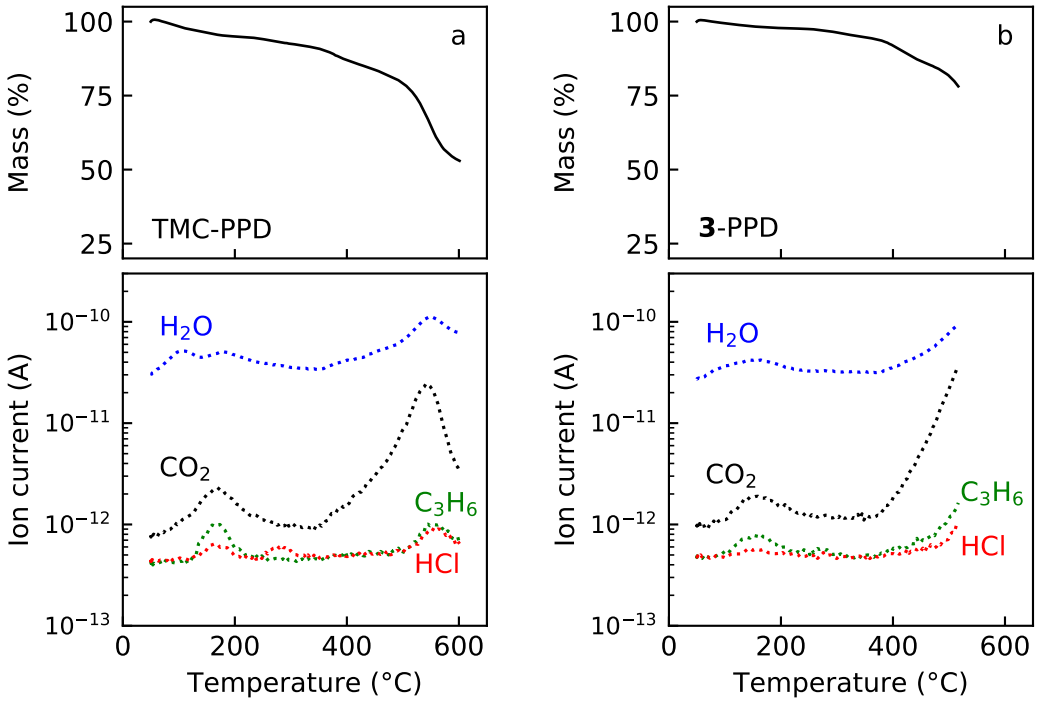

Figure 9: TGA-MS spectra of (a) TMC-PPD and (b) **2**-PPD obtained under a nitrogen atmosphere with a heating rate of 10 °C min^{-1}. The top graphs show the mass loss as function of temperature. The bottom graphs show the evolved gases. The tracked *m/z* values are H_2O (*m/z*=18, blue, —), HCl (*m/z*=38, red, —), C_3H_3 (*m/z*=39, fragment originating from aromatic ring, green, —), and CO_2 (*m/z*=44, black, —).

6. Scanning electron microscopy

Top-view scanning electron micrographs of a bare PAN support are given in Figure 10.

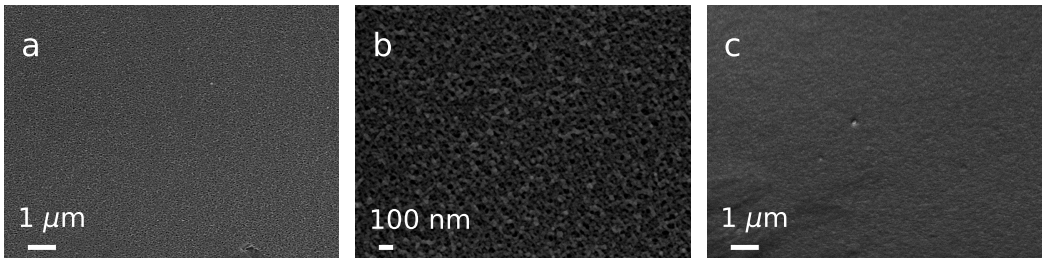

Figure 10: Top-view scanning electron micrographs of a PAN microfiltration support. (a) 10.000x magnification, (b) 50.000x magnification, and (c) 10.000x magnification with a stage angle of 45°

7. Clean water permeance

Figure 11 shows the water flux as function of transmembrane pressure (TMP) for all membranes. All membranes show a linear dependence of the flux on the TMP, where all fits pass through the origin.

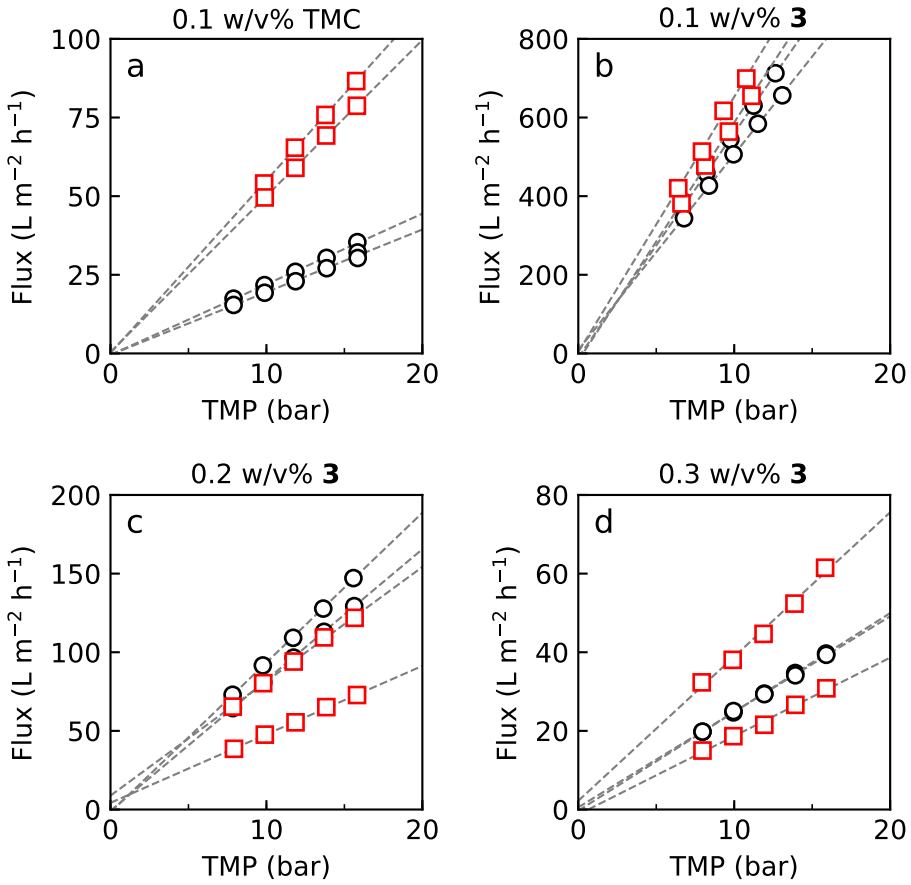

Figure 11: The clean water permeance for (a) 0.1 w/v% TMC, (b) 0.1 w/v% **3**, (c) 0.2 w/v% **3**, and (d) 0.3 w/v% **3**. MPD-based membranes are represented by red squares (□) and PPD-based membranes by black circles (○).

References

[1] L. Li, S. Zhang, X. Zhang, G. Zheng, Polyamide thin film composite membranes prepared from 3,4',5-biphenyl triacyl chloride, 3,3',5,5'-biphenyl tetraacyl chloride and m-phenylenediamine, Journal of Membrane Science 289 (2007) 258 – 267.

[2] S.-T. Kao, S.-H. Huang, D.-J. Liaw, W.-C. Chao, C.-C. Hu, C.-L. Li, D.-M. Wang, K.-R. Lee, J.-Y. Lai, Interfacially polymerized thin-film composite polyamide membrane: positron annihilation spectroscopic study, characterization and pervaporation performance, Polymer Journal 42 (2010) 242 EP –.

[3] T. Wang, L. Dai, Q. Zhang, A. Li, S. Zhang, Effects of acyl chloride monomer functionality on the properties of polyamide reverse osmosis (ro) membrane, Journal of Membrane Science 440 (2013) 48 – 57.